Eur. Phys. J. B **62**, 77–86 (2008)
DOI: 10.1140/epjb/e2008-00115-0

THE EUROPEAN PHYSICAL JOURNAL B

# Fluid friction in incompressible laminar convection: Reynolds' analogy revisited for variable fluid properties

S.P. Mahulikar[1,a] and H. Herwig[2]

[1] Department of Aerospace Engineering, Indian Institute of Technology, Bombay, Mumbai 400 076, India
[2] Institut für Thermofluiddynamik, Technische Universität Hamburg-Harburg, 21 073 Hamburg, Germany

Received 19 August 2007 / Received in final form 17 December 2007
Published online 19 March 2008 – 

**Abstract.** The Reynolds' analogy between the Stanton number ($St$) and the skin friction coefficient ($c_f$) is popularly believed to hold when $St$ increases with increasing $c_f$, for simple situations. In this investigation, the validity of Reynolds' analogy between $St$ and $c_f$ for micro-convection of liquids with variations in fluid properties is re-examined. It is found that the Sieder-Tate's property-ratio method for obtaining Nusselt number corrections is theoretically based on the validity of Reynolds' analogy. The inverse dependence of Reynolds number and skin friction coefficient is the basis for validity of the Reynolds' analogy, in convective flows with fluid property variations. This leads to the unexpected outcome that Reynolds' analogy now results in $St$ increasing with decreasing $c_f$. These results and their analyses indicate that the validity of Reynolds' analogy is based on deeper foundations, and the well-known validity criterion is a special case.

**PACS.** 44.15.+a Channel and internal heat flow – 44.27.+g Forced convection

## 1 Introduction

The effect of fluid viscosity variations on forced convective heat transfer was first modeled by Sieder and Tate [1] in 1936. They used a correction factor to the Nusselt number ($Nu$), which is the ratio of dynamic viscosity at wall ($\mu_w$) and at bulk mean fluid temperature ($\mu_m$) raised to exponent $m$. Thus, Sieder-Tate correlation, which hitherto is believed to be purely empirical, is given as,

$$(Nu/Nu_{CP}) = (\mu_m/\mu_w)^m; \quad (1)$$

where, $m \sim 0.14$, and $Nu_{CP}$ is the Nusselt number for constant fluid properties. Later, Herwig [2] and Herwig et al. [3] analyzed the influence of variable fluid properties on $Nu$ for laminar fully developed flows. Their analyses were within the framework of an asymptotic theory, which is applicable for small heat flux ($q''_w$) and high Reynolds numbers ($Re$). However, micro-convection is characterized by high $q''_w$ and low $Re$; hence, the temperature gradients are much steeper. Therefore, the effects of variations in fluid properties are much stronger, which necessitates the consideration of additional physical mechanisms that significantly affect $Nu$ [4–7]. Investigations by Mahulikar & Herwig [5,6] report physical effects in micro-convection due to variations in $\mu$ and thermal conductivity ($k$) of incompressible fluid (water). Physical effects in micro-convection due to variations in density ($\rho$) of compressible fluid (air) are reported by Mahulikar et al. [4]. Physical effects due to variations in $\mu$ and $k$ of air in conjunction with variations in $\rho$ are reported by Mahulikar and Herwig [7].

Experiments for obtaining the Fanning friction factor ($f$) for different $Re$ in microchannels are reported by Harley et al. [8]. The prime objective of their study was a comparison with results expected for the conventionally-sized channels. Three-dimensional (3-D) numerical computations of laminar water flow in heated microchannels were conducted by Toh et al. [9]. They reported that heat input lowers the frictional losses particularly at low $Re$, due to a decrease in $\mu$. The numerical results of Nonino et al. [10] confirmed that in laminar forced convection, the effects of temperature dependence of $\mu$ on $f$ cannot be ignored. Mahulikar et al. [11] arrived at the need for an investigation to examine the effect of variations in fluid properties on $f$ and $St$, in view of the validity of the Reynolds' analogy.

### 1.1 Scope of this investigation

The Reynolds' analogy between the skin friction coefficient ($c_f$) and Stanton number ($St$) for convective flows with variations in fluid properties is re-examined. In particular, the qualitative trend of $St$ changing with $c_f$ is examined in micro-convective flow, which is characterized by strong variations in fluid properties. The convective-flow situations considered give regions of validity of the Reynolds' analogy, which is attributed to a physical basis.

[a] e-mail: spm@aero.iitb.ac.in

Reynolds' analogy has been revisited in the past, e.g. for studying the minimum-dissipation transport enhancement by flow destabilisation [12].

## 2 Problem formulation and definition

The $c_f$ definition is based on the shear stress at wall ($\tau_w$) and dynamic pressure ($\frac{1}{2}\rho u_m^2$) as $c_f = \tau_w/(\frac{1}{2}\rho u_m^2)$, where $\tau_w = \mu_w(\partial u/\partial r)_w$; and the subscript 'm' refers to the mean value. The $St$ is defined based on the convective heat transfer coefficient ($h$) as $St = h/(\rho u_m c_p)$, where $c_p$ is the specific heat at constant pressure. For internal flows, $f$ is defined based on the pressure gradient along the flow $(dp/dz)$ as, $f = (dp/dz)D/(\frac{1}{2}\rho u_m^2)$, where $D$ is the circular tube diameter. When the pressure is uniform over the cross-section, i.e. $(dp/dr) = 0$, $(dp/dz)$ is related to $\tau_w$ as, $(dp/dz) = 4\tau_w/D$. This also implies that pressure change is solely due to entropy generation resulting from viscous dissipation; thus, $f = 4c_f$. Therefore, for laminar fully developed flow, $c_f = 16/Re_D$, i.e. qualitatively,

$$c_f Re_D = \text{const.} \tag{2}$$

and the relation, $St = Nu/(RePr)$ reduces to,

$$St = [Nu/(16Pr)]c_f. \tag{3}$$

For the Constant Wall Heat Flux (CWHF) and Constant Wall Temperature boundary conditions (BCs), $Nu$ = const. holds. Therefore, for a constant Prandtl number ($Pr$), $St$ increases with increasing $c_f$, and Reynolds' analogy qualitatively holds for constant fluid properties. The actual form can differ from the Reynolds' analogy for external flows for $Pr \approx 1$, i.e. $St = c_f/2$ (e.g. Ref. [13]). It is popularly believed that qualitatively, $St$ increases with increasing $c_f$ for Reynolds' analogy to be valid. The validity of Reynolds' analogy is understood to imply that convective heat transfer is more effective at the cost of increased fluid friction. As an illustration, reducing $D$ improves the effectiveness of convective heat transfer (due to an increase in $h$) at the cost of an increase in pressure drop (due to increase in $c_f$). It is popularly believed that Reynolds' analogy is invalid for liquids (since $Pr \neq 1$), and especially so when variations in fluid properties are considered [14].

### 2.1 Re-examination of Reynolds' analogy for variable fluid properties

The relation between $c_f$ and $Re$ (both are flow parameters) and the relation between the convective heat transfer performance and skin friction are now analysed. The case of an inverse dependence of $c_f$ and $Re$ given by equation (2), with $Re_D = \rho u_m D/\mu_m$, reduces to,

$$(D/u_m)[(\mu_w/\mu_m)(du/dr)_w] = \text{const.} \tag{4}$$

Equation (4) includes $\mu$-variations over the cross-section; therefore, both $\mu_w$ and $\mu_m$ are incorporated. For steady incompressible flow through a tube of constant $D$, equation (4) reduces to,

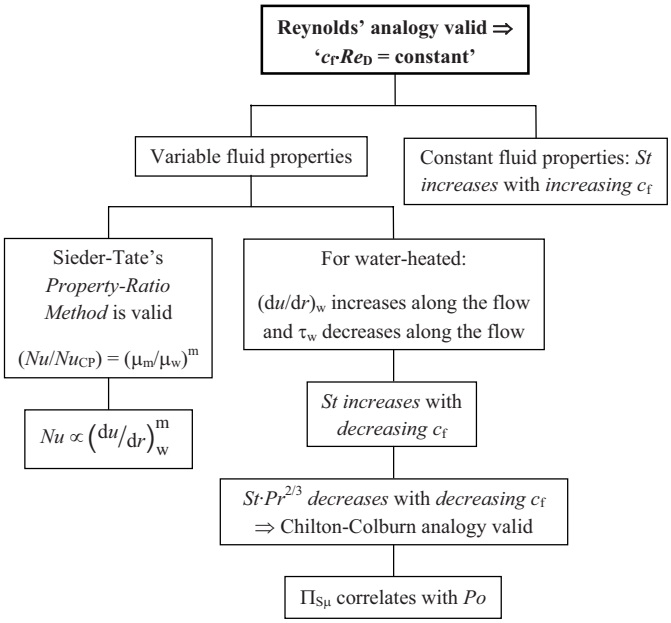


**Fig. 1.** Reynolds' analogy for constant and variable properties of incompressible fluid.

$$(du/dr)_w \propto (\mu_m/\mu_w). \tag{4.1}$$

For water-heated, $\mu_m > \mu_w$, hence, $(du/dr)_w$ is higher than for the parabolic $u(r)$-profile with, '$\mu_m = \mu_w$'; and for the same $u_m$, $u(r)$-profile is flattened compared to the '$\mu_m = \mu_w$' case. The $(du/dr)_w$ in equation (4.1) also influences $St$ and $Nu$, because flatter $u(r)$-profiles increase $Nu$ relative to the parabolic $u(r)$-profile; thus, $T_w$ is reduced for given $T_m$ and $q''_w$. Comparing equations (1) and (4.1), the estimation of $Nu$ based on the property-ratio method of Sieder & Tate [1] given by equation (1) is now theoretically explained. Further, $(Nu/Nu_{CP}) = [(du/dr)_w/(du/dr)_{w,CP}]^m$; where, $(du/dr)_{w,CP} = -4u_m/R$, which implies that $Nu \propto [(du/dr)_w]^m$. Thus, $Nu$ is proportional to the wall velocity gradient raised to the same exponent '$m$' as in the Sieder-Tate correlation [Eq. (1)]. Multiplying equation (4.1) by $\mu_w$ gives,

$$\tau_w \propto \mu_m; \tag{4.2}$$

therefore, the decrease in $\mu_m$ along the flow for the case of water-heated causes $c_f$ to decrease, when Reynolds' analogy is valid. From equations (4.1) and (4.2), the Reynolds' analogy for variable fluid properties is now valid when $St$ increases with decreasing $c_f$. Since convective heat transfer effectiveness and skin friction are both embedded in $c_f$, equation (2) is the basis for Reynolds' analogy when variations in fluid properties are considered. Therefore, from equation (3), the parameter, $(StPr/Nu)$ [$=(1/Re)$] versus $c_f$ should be plotted, and Reynolds' analogy is qualitatively valid when $Re$ and $c_f$ are inversely dependent. Figure 1 consolidates the implications resulting from the validity of Reynolds' analogy when variations in incompressible fluid properties are considered.

Laminar flow of water is now numerically considered, in which variations in fluid properties have a significant

influence on the micro-convective heat transfer characteristics [6]. For water in the temperature range 0–100 °C, $\mu(T)$ varies by 84%, $k(T)$ by 21%, $\rho(T)$ by 4%, and $c_p(T)$ by 1% (e.g. Ref. [15]). Because $\rho(T)$ and $c_p(T)$ variations are insignificant relative to $\mu(T)$ and $k(T)$ variations, this investigation assumes invariant $\rho$ and $C_p$.

## 2.2 Conservation equations

The following steady state continuum-based incompressible laminar conservation equations for 2-D with axisymmetry, as elaborated in Mahulikar and Herwig [5] are numerically solved.

### 2.2.1 Continuity equation [considering radial (r-direction) flow]

(i) Dimensional form

$$(v/r) + (\partial v/\partial r) + (\partial u/\partial z) = 0. \tag{5}$$

(ii) Dimensionless form

$$(\bar{v}/\bar{r}) + (\partial \bar{v}/\partial \bar{r}) + (\partial \bar{u}/\partial \bar{z})/2 = 0; \tag{5.1}$$

where, $\bar{u} = u/u_m, \bar{v} = v/u_m, \bar{z} = z/D$, and $\bar{r} = r/R$.

### 2.2.2 Axial (z-direction)-momentum equation

(i) Dimensional form

$$\rho[v(\partial u/\partial r) + u(\partial u/\partial z)] = -(\partial p/\partial z) + [(\mu/r) + (\partial \mu/\partial r)][(\partial u/\partial r) + (\partial v/\partial z)] + \mu[2(\partial^2 u/\partial z^2) + (\partial^2 u/\partial r^2) + (\partial^2 v/\partial r \cdot \partial z)] + 2(\partial \mu/\partial z)(\partial u/\partial z). \tag{6}$$

(ii) Dimensionless form

$$2\bar{v}(\partial \bar{u}/\partial \bar{r}) + \bar{u}(\partial \bar{u}/\partial \bar{z}) = -\frac{1}{2}(\partial \bar{p}/\partial \bar{z}) + (2/Re_D) \cdot [(\bar{\mu}/\bar{r}) + \bar{S}_\mu \Pi_{S\mu}(\partial \theta/\partial \bar{r})][2(\partial \bar{u}/\partial \bar{r}) + (\partial \bar{v}/\partial \bar{z})] + (2\bar{\mu}/Re_D)\left[(\partial^2 \bar{u}/\partial \bar{z}^2) + 2(\partial^2 \bar{u}/\partial \bar{r}^2) + \frac{\partial^2 \bar{v}}{\partial \bar{r}\partial \bar{z}}\right] + (2\bar{S}_\mu/Re_D)\Pi_{S\mu}(\partial \theta/\partial \bar{z})(\partial \bar{u}/\partial \bar{z}); \tag{6.1}$$

where, $\bar{p} = p/(\frac{1}{2}\rho u_m^2), \bar{\mu} = \mu/\mu_m, \bar{S}_\mu = S_\mu/S_{\mu m}$ $(S_\mu = \partial \mu/\partial T)$.

### 2.2.3 Radial (r-direction)-momentum equation

(i) Dimensional form

$$\rho[\nu(\partial \nu/\partial r) + u(\partial \nu/\partial z)] = -(\partial p/\partial r) + 2[(\mu/r) + (\partial \mu/\partial r)](\partial \nu/\partial r) - (\mu \nu/r^2) + \mu[(\partial^2 \nu/\partial z^2) + 2(\partial^2 \nu/\partial r^2) + (\partial^2 u/\partial r \partial z)] + (\partial \mu/\partial z)[(\partial \nu/\partial z) + (\partial u/\partial r)]. \tag{7}$$

(ii) Dimensionless form

$$2\bar{\nu}(\partial \bar{\nu}/\partial \bar{r}) + \bar{u}(\partial \bar{\nu}/\partial \bar{z}) = -(\partial \bar{p}/\partial \bar{r}) + (8/Re_D) \cdot [(\bar{\mu}/\bar{r}) + \bar{S}_\mu \Pi_{S\mu}(\partial \theta/\partial \bar{r})](\partial \bar{\nu}/\partial \bar{r}) + (\bar{\mu}/Re_D) \cdot \left[(\partial^2 \bar{\nu}/\partial \bar{z}^2) - 4(\bar{\nu}/\bar{r}^2) + 8(\partial^2 \bar{\nu}/\partial \bar{r}^2) + 2\left(\frac{\partial^2 \bar{u}}{\partial \bar{r}\partial \bar{z}}\right)\right] + (\bar{S}_\mu/Re_D)\Pi_{S\mu}(\partial \theta/\partial \bar{z})[(\partial \bar{\nu}/\partial \bar{z}) + 2(\partial \bar{u}/\partial \bar{r})]. \tag{7.1}$$

### 2.2.4 Energy equation

(i) Dimensional form

$$\rho c_p[\nu(\partial T/\partial r) + u(\partial T/\partial z)] = [(k/r) + (\partial k/\partial r)] \cdot (\partial T/\partial r) + k(\partial^2 T/\partial r^2) + (\partial k/\partial z) \cdot (\partial T/\partial z) + k(\partial^2 T/\partial z^2). \tag{8}$$

(ii) Dimensionless form

$$Pe_D[2\bar{\nu}(\partial \theta/\partial \bar{r}) + \bar{u}(\partial \theta/\partial \bar{z})] = 4[(\bar{k}/\bar{r}) + \bar{S}_k \Pi_{Sk} \cdot (k_m/k_{m,in})(\partial \theta/\partial \bar{r})](\partial \theta/\partial \bar{r}) + \bar{k}[4(\partial^2 \theta/\partial \bar{r}^2) + (\partial^2 \theta/\partial \bar{z}^2)] + \Pi_{Sk}\bar{S}_k(k_m/k_{m,in})(\partial \theta/\partial \bar{z}^2); \tag{8.1}$$

where, $\theta = k_{m,in}(T - T_{m,in})/(q''_w D), Pe_D = Re_D Pr, \bar{k} = k/k_m$, and $\bar{S}_k = S_k/S_{km} (S_k = \partial k/\partial T)$.

Though the dimensional forms of the governing equations are solved, the dimensionless forms are presented to better illustrate the convective-flow physics. The momentum and energy equations are mutually coupled, because $\mu(T)$-variations and radial flow ($\nu \neq 0$) induced by $\mu(r, z)$-variations are incorporated. In equations (6.1), (7.1), and (8.1), the dimensionless groups, $\Pi_{S\mu} = S_{\mu m} q''_w D/(\mu_m k_m)$ and $\Pi_{Sk} = S_{km} q''_w D/k_m^2$, represent the ratio of variation in properties to the properties. High values of $\Pi_{S\mu}$and $\Pi_{Sk}$ denote strong effects due to variations in fluid properties on convective flow characteristics. These groups are the product of temperature perturbation parameter $[=f(q''_w D/k)]$ and dimensionless property sensitivities, $S_\mu(T/\mu)$ and $S_k(T/k)$ [2]. Their significance is the ratio of Brinkman numbers ($Br$), which are based on the ratio of momentum transfer to heat conduction in the fluid [5].

## 2.3 Boundary conditions (BCs)

The following flow and thermal BCs are applied to the computational domain:

(i) The BCs of symmetry are applied at the axis of the micro-tube ($r = 0$); therefore, $\nu = (\partial u/\partial r) = (\partial p/\partial r) = (\partial T/\partial r) = 0$. In dimensionless form, they are respectively given as (for $\bar{r} = 0$): $\bar{\nu} = (\partial \bar{u}/\partial \bar{r}) = (\partial \bar{p}/\partial \bar{r}) = (\partial \theta/\partial \bar{r}) = 0$.

(ii) The no-slip and no normal flow BCs are applied at the non-porous rigid wall ($r = R$), i.e. $u_w = \nu_w = 0$; and for the applied heat flux at the wall, $(\partial T/\partial r)_w = q''_w/k_w$. In dimensionless form, they are respectively given as (for $\bar{r} = 1$): $\bar{u}_w = \bar{\nu}_w = 0$; and $(\partial \theta/\partial \bar{r})_w = \frac{1}{2}(k_m/k_w)$.

(iii) At the inlet-upstream location ($z = 0^-$), laminar fully-developed flow BCs for constant fluid properties are used. Hence, the inlet $u$-profile is given as, $u(r, 0^-) = 2u_m(1 - \bar{r}^2)$; and the inlet $T$-profile for CWHF BC is given as, $T(r, 0^-) = T_{0,in} + (q''_w R/k)[\bar{r}^2 - (\bar{r}^4/4)]$ (where, $T_{0,in} = 20$ °C). In dimensionless form, they are given as (for $\bar{z} = 0^-$), $\bar{u}(\bar{r}, 0^-) = 2(1 - \bar{r}^2)$, and $\theta(\bar{r}, 0^-) = \frac{1}{2}[\bar{r}^2 - (\bar{r}^4/4) - \frac{7}{24}]$. From the inlet location onwards and up to the exit [$z = 0^+$ to $z = L$, i.e. $\bar{z} = 0^+$ to $\bar{z} = (L/D)$], $\mu(T)$ and $k(T)$ variations are switched on.

(iv) At the exit-plane, the only variable whose value is specified is, $p_{ex} = p_{atm} = 1.013 \times 10^5$ Pa (I.S.A. pressure). Neumann boundary conditions are imposed on the other transport variables $(u, \nu, T)$, i.e. the rates of change of their dimensionless profiles along the flow are equated to zero. The downstream gradient of $u$ is zero, due to the assumption of fully-developed flow at the exit (which is exact for $Re_D \to 0$). This results in, $\nu_{ex} = 0$, thereby also imposing the $\nu$-gradient at the exit-plane and its' downstream to zero.

## 3 Numerical solution and inference from theoretical analysis

The computational domain comprises a circular microtube with radius, $R = 50$ $\mu$m, and length, $L = 5$ mm [$(L/D) = 50$]. Equations (5–8), with BCs are simultaneously solved by 2nd-order accurate Implicit Finite-Volume differencing scheme. The 'Semi-Implicit Method for Pressure-Linked Equations', i.e. SIMPLE pressure-differencing scheme is used for obtaining pressure distribution. Graded mesh with 10 000 cells [= 200 (axial)×50 (radial), $(\Delta z/\Delta r) = 25$] with finer grid spacing in the vicinity of the inlet and the wall, is used. This grid density is conservatively selected based on grid independency of the final results ($St$ and $c_f$ values). Also, diminishing returns were observed as the grid density was increased towards $200 \times 50$, in terms of computational time and accuracy of the numerical results. Because axial temperature gradients are less critical than radial, the computational cells have a high aspect ratio [$(\Delta z/\Delta r) = 25$]. Increasing the number of grid points in the axial direction to make, $(\Delta z/\Delta r) \to 1$, results in unreasonably high computational effort and time. The maximum deviations in $St$ and $c_f$ results for grids, $200 \times 50$ [$(\Delta z/\Delta r) = 25$], $250 \times 40$ [$(\Delta z/\Delta r) = 16$], $180 \times 50$ [$(\Delta z/\Delta r) = 27.8$], and $200 \times 45$ [$(\Delta z/\Delta r) = 22.5$], are less than 0.05%. Additional details pertaining to the convergence of solution, accuracy of the numerical results, and validation with benchmark cases for constant fluid properties are in [6] .

Water is one of the most representative liquids that have high $S_\mu$; using a different liquid with different $S_\mu$ but the same sign is expected to change the results only quantitatively. In this investigation, the quantitative results are unimportant, as inferences are based exclusively on their trends. The $\mu(T)$ in kg/ms for single-phase water is given as (Ref. [16]),

$$\mu(T) = \mu(T_{ref})(T/T_{ref})^n \exp[B(T^{-1} - T_{ref}^{-1})]; \quad (9)$$

where, $n = 8.9$, $B = 4700$, and $\mu(T_{ref}) = 1.005 \times 10^3$ kg/ms at $T_{ref} = 293$ K. The $k(T)$ in W/mK for single-phase water is given by cubic fit as, $k(T) = -1.51721 + 0.0151476\,T - 3.5035 \times 10^{-5}\,T^2 + 2.74269 \times 10^{-8}\,T^3$. This variation is obtained as a least-square-error fit of data from Holman [15] in the operating temperature range 274–372 K. Incorporating $\mu(T)$ and $k(T)$ variations for water, results are generated for $u(r, z)$, $\nu(r, z)$, and $T(r, z)$ profiles; and the variations of $St$, $Pr$, $c_f$, and $Re$ along the flow are deduced.

Table 1a gives $c_{f,in}$, $c_{f,max}$, and $c_{f,ex}$, $Re_{in}$ and $Re_{ex}$, and $St_{in}$ and $St_{ex}$, for $u_m$ =0.05, 0.75, 1.5, 2.5, and 3.0 m/s, for various allowable $q''_w$ for single-phase flow. Figure 2 gives $(1/Re)$ versus $c_f$ for $u_m = 0.05$, 1.5, and 3.0 m/s, for different $q''_w$; for examining Reynolds' analogy.

Figure 3 gives $St$ versus $c_f$ for the same cases as in Figure 2, which indicates reversed trends of variations of $St$ versus $c_f$ and $(1/Re)$ versus $c_f$. The $St$ increases along the flow; but $c_f$, which depends on '$\mu_w(\partial u/\partial r)_w$' first increases, reaches a maximum ($c_{f,max}$) at axial location $z_{cf,max}$, and then decreases (Fig. 4). The $\mu_w$ decreases for water-heated [Eq. (9)]; and $(\partial u/\partial r)_w$ first increases, reaches a maximum $[(\partial u/\partial r)_{w,max}]$ at axial location $z_{ugw,max}$, and then decreases along the flow (Fig. 5). The variation in $(\partial u/\partial r)_w$ is due to flattening of the initially parabolic $u(r)$-profile, due to hydrodynamic-undevelopment of flow [17]. Table 1b lists $\bar{z}_{cf,max}$ and $\bar{z}_{ugw,max}$ for the same $u_m$ and $q''_w$ as in Table 1a; which shows that $\bar{z}_{cf,max} < \bar{z}_{ugw,max}$ , because $(\partial u/\partial r)_w$ trend is retarded by $\mu_w$-decrease along the flow.

The Reynolds' analogy would be popularly believed to be invalid when $St$ decreases with increasing $c_f$; since, for constant fluid properties, $St \propto c_f$ [Ref. Eq. (3)]. This behavior is observed over most of the flow field for low $u_m$ (low $Re_D$), as indicated by Figure 3a. But from Figure 2a, because $Re$ and $c_f$ are inversely dependent over a significant percentage of the flow regime, Reynolds' analogy for variable fluid properties is predominantly valid. Figure 6 shows the variation of $St\,Pr^{2/3}$ versus $c_f$, which is the parameter in the Chilton-Colburn analogy [18] that also considers the variation, $Pr(T)$. The Chilton-Colburn analogy is also largely valid (qualitatively) in Figure 6a, and its' validity in Figure 6c is questionable. Therefore, the Chilton-Colburn analogy of $St\,Pr^{2/3}$ increasing with increasing $c_f$ is qualitatively valid when $St$ increases with decreasing $c_f$.

Figures 2, 3, and 6 illustrated the analogies and their validities considering both $\mu(T)$ and $k(T)$ variations. For illustrating the role of $\mu(T)$-variation only, Figure 7 illustrates the variations of the following (for $u_m$ =0.75 m/s and $q''_w = \pm 10$ and $\pm 30$ W/cm$^2$): ($a$) $1/Re$ versus $c_f$, ($b$) $St$ versus $c_f$, and ($c$) $St\,Pr^{2/3}$ versus $c_f$. It is seen that qualitatively, the trends of validity of the Reynolds' analogy are the same as when both $\mu(T)$ and $k(T)$ variations are considered.

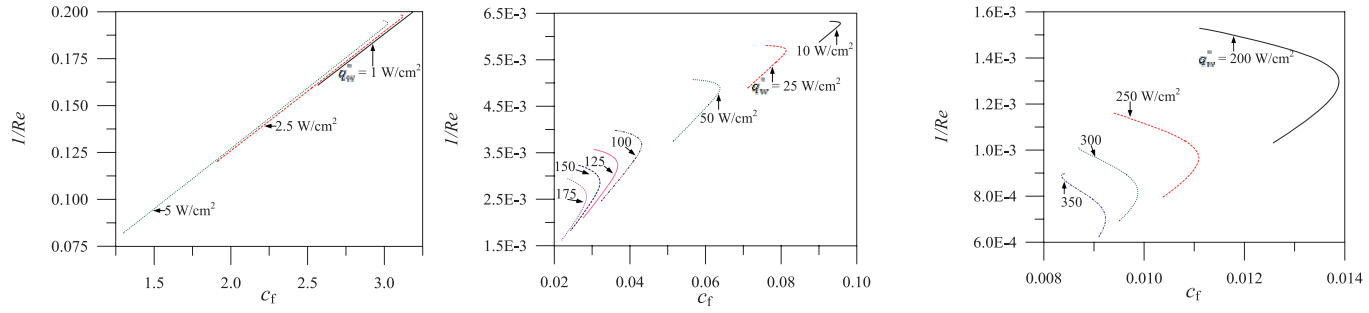


(*a*) $u_m$ = 0.05 m/s (Reynolds' analogy largely valid). (*b*) $u_m$ = 1.5 m/s. (*c*) $u_m$ = 3.0 m/s (Reynolds' analogy largely invalid).

(a) (b) (c)

**Fig. 2.** Variation of $(1/Re)$ versus $c_f$. (a) 0.05 m/s (Reynolds' analogy largely valid). (b) $u_m$ = 1.5 m/s. (c) $u_m$ = 3.0 m/s (Reynolds' analogy largely invalid).

**Table 1.** Variation of convective flow parameters with $u_m$ and $q''_W$.

(a) $Re$, $c_f$, and $St$

| $u_m$ (m/s) | $q''_W$ (W/cm$^2$) | $Re_{in}, Re_{ex}$ | $c_{f,in}, c_{f,max}, c_{f,ex}$ | $St_{in}, St_{ex}$ |
|---|---|---|---|---|
| 0.05 | 1.0 | 5, 6 | 3.179, 3.185, 2.568 | 0.127, 0.133 |
| | 2.5 | 5, 8 | 3.109, 3.123, 1.909 | 0.127, 0.138 |
| | 5.0 | 5, 12 | 2.997, 3.024, 1.291 | 0.127, 0.145 |
| 0.75 | 10 | 79, 91 | 0.186, 0.191, 0.168 | 0.0085, 0.0089 |
| | 25 | 86, 119 | 0.152, 0.162, 0.123 | 0.0085, 0.0093 |
| | 50 | 99, 172 | 0.114, 0.127, 0.082 | 0.0086, 0.0098 |
| | 75 | 112, 227 | 0.089, 0.103, 0.062 | 0.0086, 0.0102 |
| | 100 | 126, 283 | 0.072, 0.086, 0.050 | 0.0087, 0.0104 |
| 1.5 | 10 | 158, 170 | 0.093, 0.096, 0.090 | 0.0042, 0.0044 |
| | 25 | 172, 204 | 0.076, 0.081, 0.071 | 0.0043, 0.0046 |
| | 50 | 197, 267 | 0.057, 0.064, 0.051 | 0.0043, 0.0048 |
| | 100 | 251, 406 | 0.036, 0.043, 0.032 | 0.0043, 0.0051 |
| | 125 | 280, 477 | 0.030, 0.037, 0.027 | 0.0043, 0.0052 |
| | 150 | 310, 547 | 0.026, 0.032, 0.024 | 0.0043, 0.0053 |
| | 175 | 340, 618 | 0.024, 0.028, 0.022 | 0.0044, 0.0053 |
| 2.5 | 10 | 263, 275 | 0.056, 0.057, 0.056 | 0.0025, 0.0026 |
| | 25 | 287, 319 | 0.046, 0.049, 0.045 | 0.0026, 0.0027 |
| | 50 | 329, 397 | 0.034, 0.038, 0.034 | 0.0026, 0.0028 |
| | 75 | 373, 481 | 0.027, 0.031, 0.027 | 0.0026, 0.0029 |
| | 100 | 419, 570 | 0.022, 0.026, 0.022 | 0.0026, 0.0030 |
| | 125 | 467, 662 | 0.018, 0.022, 0.019 | 0.0026, 0.0031 |
| | 150 | 516, 753 | 0.016, 0.019, 0.017 | 0.0026, 0.0031 |
| | 175 | 567, 843 | 0.014, 0.017, 0.015 | 0.0026, 0.0032 |
| | 200 | 619, 935 | 0.013, 0.015, 0.014 | 0.0026, 0.0032 |
| | 250 | 722, 1113 | 0.011, 0.013, 0.012 | 0.0026, 0.0032 |
| | 300 | 825, 1268 | 0.010, 0.012, 0.011 | 0.0027, 0.0032 |
| 3.0 | 200 | 654, 970 | 0.0111, 0.0139, 0.0126 | 0.0021, 0.0026 |
| | 250 | 861, 1256 | 0.0094, 0.0111, 0.0104 | 0.0022, 0.0027 |
| | 300 | 990, 1445 | 0.0087, 0.0099, 0.0095 | 0.0022, 0.0027 |
| | 350 | 1114, 1601 | 0.0084, 0.0092, 0.0091 | 0.0022, 0.0027 |

(b) $\bar{z}_{cf,max}$ and $\bar{z}_{ugw,max}$

| $u_m$(m/s) | $q''_w$(W/cm$^2$) | $\bar{z}_{cf,max}$ | $\bar{z}_{ugw,max}$ |
|---|---|---|---|
| 0.05 | 1.0 | 0.3605 | 1.468 |
| | 2.5 | 0.3605 | 1.468 |
| | 5.0 | 0.3605 | 0.927 |
| 0.75 | 10 | 2.5040 | 6.355 |
| | 25 | 2.6910 | 6.355 |
| | 50 | 2.9798 | 5.689 |
| | 75 | 3.3808 | 5.819 |
| | 100 | 3.6939 | 6.355 |
| 1.5 | 10 | 4.3538 | 13.107 |
| | 25 | 5.1838 | 11.660 |
| | 50 | 5.8192 | 11.268 |
| | 100 | 7.2058 | 11.860 |
| | 125 | 7.9617 | 12.472 |
| | 150 | 8.5987 | 12.893 |
| | 175 | 9.0961 | 13.542 |
| 2.5 | 10 | 7.9617 | 22.068 |
| | 25 | 8.5987 | 22.068 |
| | 50 | 9.9645 | 18.775 |
| | 75 | 10.8847 | 19.057 |
| | 100 | 11.8597 | 19.632 |
| | 125 | 13.1066 | 22.068 |
| | 150 | 14.2139 | 22.068 |
| | 175 | 15.3870 | 22.068 |
| | 200 | 16.6302 | 22.068 |
| | 250 | 18.4960 | 24.392 |
| | 300 | 20.8217 | 25.092 |
| 3.0 | 200 | 18.7751 | 25.448 |
| | 250 | 22.0678 | 29.242 |
| | 300 | 24.7401 | 30.469 |
| | 350 | 29.6462 | 30.469 |

### 3.1 Interpretation based on theorem of minimum entropy production

Increasing $(du/dr)_w$ decreases entropy generation due to heat transfer ($\dot{S}_{gen,therm}$) by increasing $St$ and $h$, which reduces $(T_w - T_m)$. However, increasing $(du/dr)_w$ increases $c_f$, which increases entropy generation due to fluid friction ($\dot{S}_{gen,visc}$) [19]. Thus, the current understanding of the validity of Reynolds' analogy is linked to $\dot{S}_{gen,therm}$ and $\dot{S}_{gen,visc}$ having compensating roles. For small changes in the system state close to equilibrium, convection and flow follow the Theorem of Minimum Entropy Production (TMEP) [20]. As per TMEP, entropy generation is small and nearly constant in non-equilibrium states in the

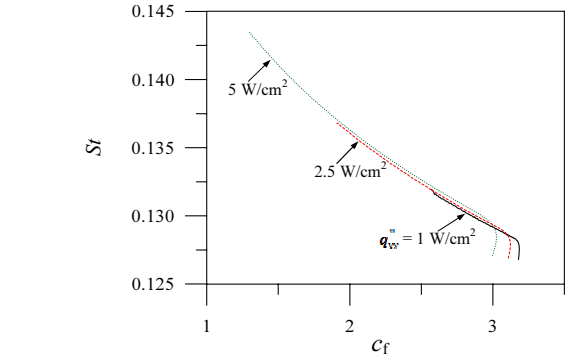


3(*a*) $u_m = 0.05$ m/s (Reynolds' analogy largely valid)

(a)

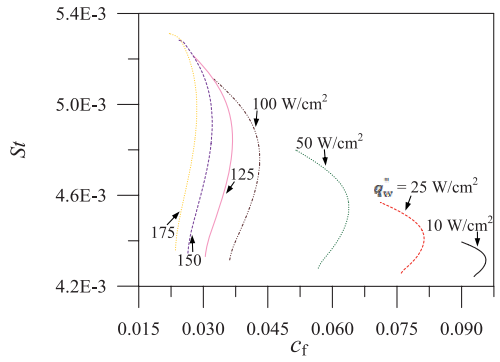


(*b*) $u_m = 1.5$ m/s.

(b)

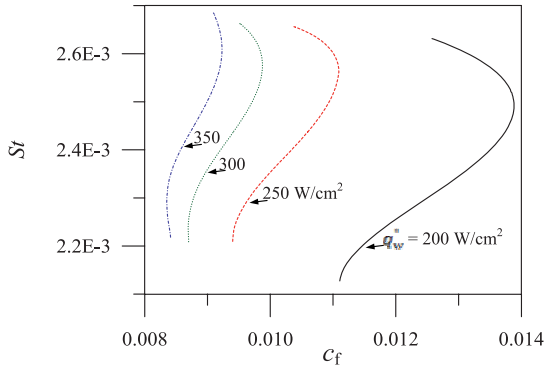


(*c*) $u_m = 3.0$ m/s (Reynolds' analogy largely invalid).

(c)

**Fig. 3.** Variation of $St$ versus $c_f$: Examination of Reynolds' analogy. (a) $u_m = 0.05$ m/s (Reynolds' analogy largely valid). (b) $u_m = 1.5$ m/s. (c) $u_m = 3.0$ m/s (Reynolds' analogy largely invalid).

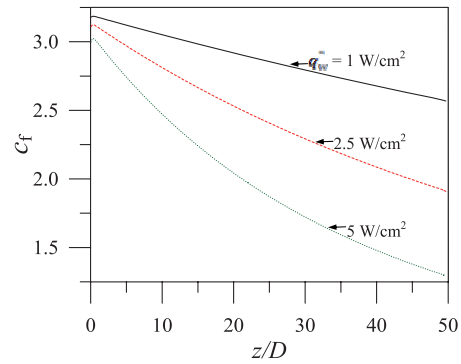


(*a*) $u_m = 0.05$ m/s.

(a)

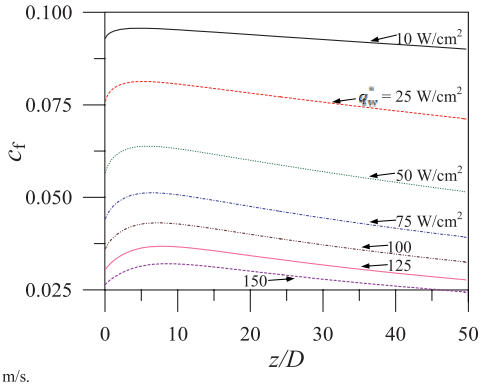


(*b*) $u_m = 1.5$ m/s.

(b)

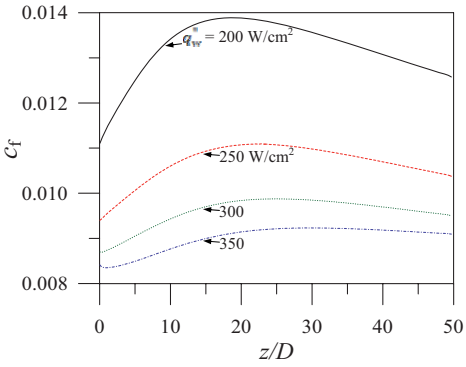


(*c*) $u_m = 3.0$ m/s.

(c)

**Fig. 4.** Variation of $c_f$ versus $\bar{z}$. (a) $u_m = 0.05$ m/s. (b) $u_m = 1.5$ m/s. (c) $u_m = 3.0$ m/s.

vicinity of equilibrium. Therefore, $\dot{S}_{gen,Tot} = \dot{S}_{gen,therm} + \dot{S}_{gen,visc}$, is nearly constant; and a change in $\dot{S}_{gen,therm}$ is nearly compensated by an opposite change in $\dot{S}_{gen,visc}$.

From $z = 0$ to $z = z_{ugw,max}$, $u$-gradients change significantly relative to the region from $z = z_{ugw,max}$ to $z = L$. This is attributed to the process of flow undevelopment from constant (prior to inlet) to variable fluid properties (inlet onwards downstream). In this region, the induced radial flow is non-negligible, and convective heat transfer is significantly influenced by radial convection [6] and $(du/dr)_w$. Therefore, TMEP is not applicable and the Reynolds' analogy is invalid from $z = 0$ to $z = z_{ugw,max}$; but after $z = z_{ugw,max}$, variations in $u$-gradients subside. Thus, Reynolds' analogy is valid when changes in field variables determined by linear constitutive laws in convective fluid flow, are small enough for TMEP to be applicable. The validity of Reynolds' analogy for small changes in field variables is corroborated by the linear asymptotic analysis of Herwig [2]. It was demonstrated that for small perturbations in fluid temperature, the results of the asymptotic approach are in agreement with the predictions based on Sieder and Tate [1]. But if these

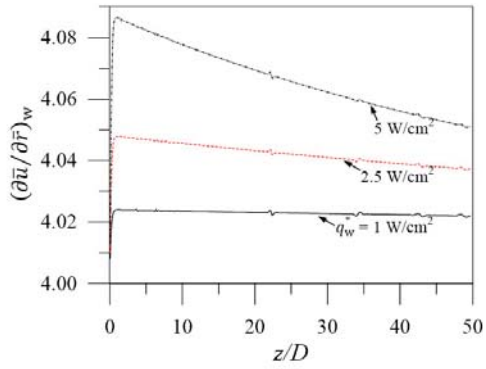


(*a*) $u_m$ = 0.05 m/s.

(a)

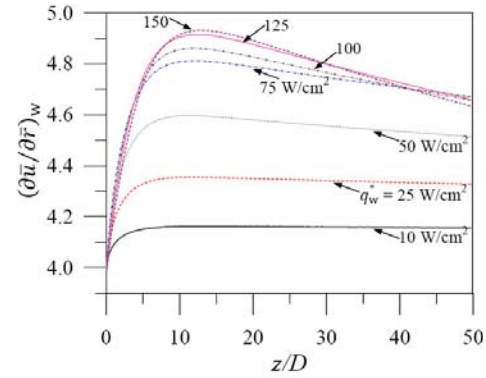


(*b*) $u_m$ = 1.5 m/s.

(b)

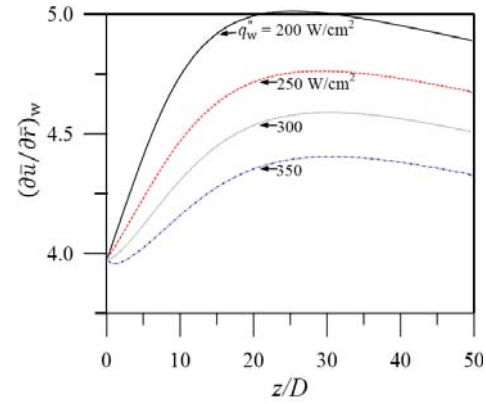


(*c*) $u_m$ = 3.0 m/s.

(c)

**Fig. 5.** Variation of $(\partial\bar{u}/\partial\bar{r})_w$ versus $\bar{z}$. (a) $u_m$ = 0.05 m/s. (b) $u_m$ = 1.5 m/s. (c) $u_m$ = 3.0 m/s.

perturbations are large, then higher order terms must also be considered in the Taylor series expansion of the fluid property variations.

## 4 Significance of additional dimensionless group, $\Pi_{S\mu}$

The $\Pi_{S\mu}$ emerged from the non-dimensionalisation of governing conservation equations [Ref. Eqs. (6.1) and (7.1)].

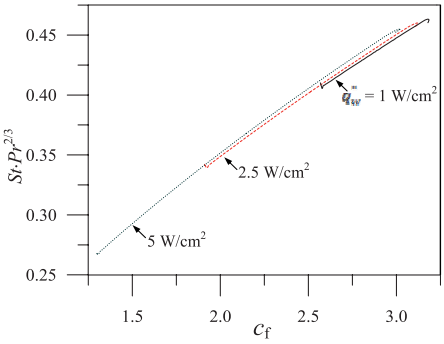


(*a*) $u_m$ = 0.05 m/s (Chilton-Colburn analogy largely valid).

(a)

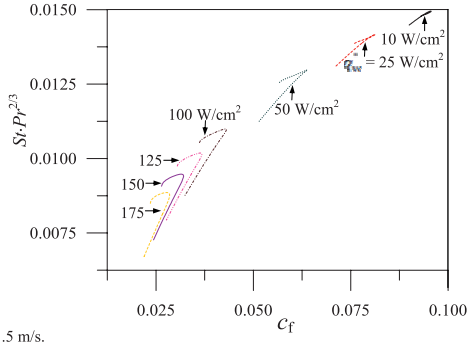


(*b*) $u_m$ = 1.5 m/s.

(b)

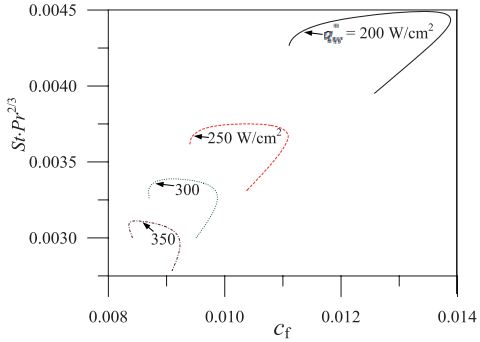


(*c*) $u_m$ = 3.0 m/s (Chilton-Colburn analogy largely invalid).

(c)

**Fig. 6.** Variation of $St\,Pr^{2/3}$ versus $c_f$: examination of Chilton-Colburn analogy. (a) $u_m$ = 0.05 m/s (Chilton-Colburn analogy largely valid). (b) $u_m$ = 1.5 m/s. (c) $u_m$ = 3.0 m/s (Chilton-Colburn analogy largely invalid).

It is also supported by a dimensional analysis for the dependence of friction factor given as,

$$f = \phi(\rho, u_m, D, \mu, k, S_\mu, q''_w); \tag{10}$$

where, $\phi$ is a mathematical function. The dimensions of the 7 parameters are given as follows: $[\rho] = [M^1L^{-3}]$, $[u_m] = [L^1T^{-1}]$, $[D] = [L^1]$, $[\mu] = [M^1L^{-1}T^{-1}]$, $[k] = [M^1L^1T^{-3}\Theta^{-1}]$, $[S_\mu] = [M^1L^{-1}T^{-1}\Theta^{-1}]$, and $[q''_w] = [M^1T^{-3}]$. The $M$, $L$, $T$, and $\Theta$, are the fundamental dimensions of mass, length, time, and temperature, respectively. Equation (10) has 7 parameters and there are 4 fundamental dimensions; hence, there are three dimensionless

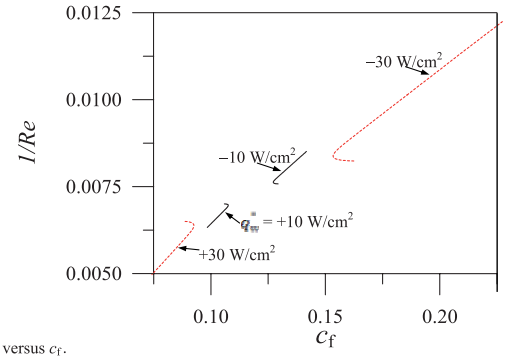


(*a*) $1/Re$ versus $c_f$.

(a)

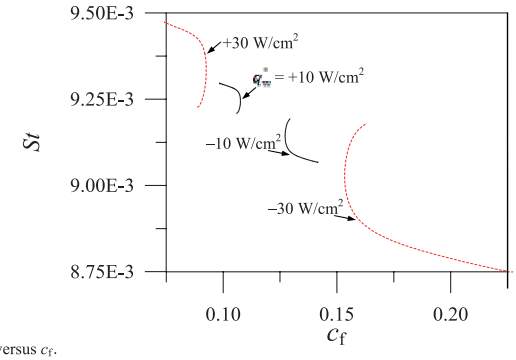


(*b*) $St$ versus $c_f$.

(b)

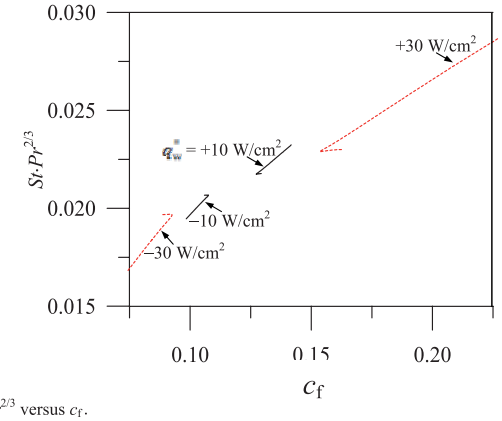


(*c*) $St{\cdot}Pr^{2/3}$ versus $c_f$.

(c)

**Fig. 7.** Examination of analogies for $u_m = 0.75$ m/s, considering $\mu(T)$-variation only. (a) $1/Re$ versus $c_f$. (b) $St$ versus $c_f$. (c) $St\,Pr^{2/3}$ versus $c_f$

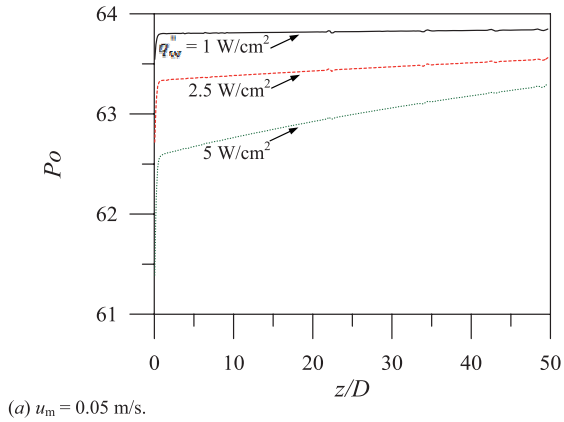


(*a*) $u_m = 0.05$ m/s.

(a)

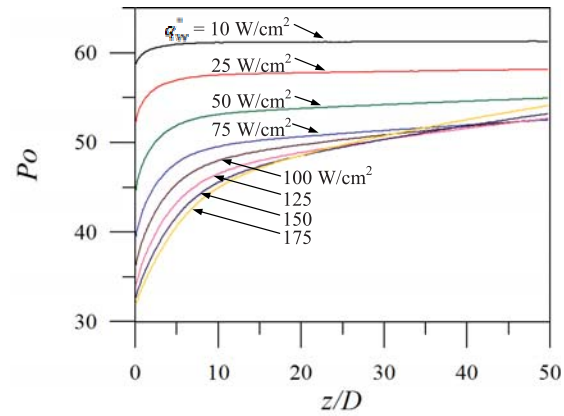


(*b*) $u_m = 1.5$ m/s.

(b)

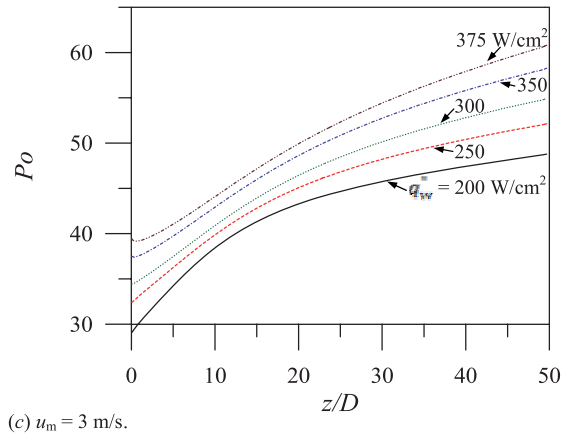


(*c*) $u_m = 3$ m/s.

(c)

**Fig. 8.** Variation of $Po$ along flow. (a) $u_m = 0.05$ m/s. (b) $u_m = 1.5$ m/s. (c) $u_m = 3$ m/s.

groups as per the Buckingham-$\Pi$ theorem. Choosing $\rho$, $u_m$, $D$, and $k$, as the recurring parameters, the 4 fundamental dimensions are expressed as, $[M] = [\rho D^3]$, $[L] = [D]$, $[T] = [D/u_m]$, and $[\Theta] = \rho u_m^3 D/k$. From the remaining 3 non-recurring parameters $\mu$, $q''_w$ and $S_\mu$, the 3 dimensionless groups are obtained as follows: $\Pi_1 = Re_D = \rho u_m D/\mu$, $\Pi_2 = Br_{qw} = \mu u_m^2/(q''_w D)$, and $\Pi_3 = Br_{S\mu} = S_\mu u_m^2/k$. The $Br_{qw}$ is Brinkman number based on $q''_w$, and $Br_{S\mu}$ is Brinkman number based on $S_\mu$ [5]; and $\Pi_{S\mu} = Br_{S\mu}/Br_{qw} = S_\mu q''_w D/(\mu k)$. This dimensional analysis and the earlier non-dimensionalisation of the conservation equations suggest the dependence given by equation (10) to reduce to the form, $f = \phi(Re_D, \Pi_{S\mu})$.

The role of $\Pi_{S\mu}$ in flow friction is now investigated considering $\mu(T)$ and $k(T)$ variations, and the variation of the Poiseuille number ($Po = f Re_D$) along the flow is studied in Figure 8. For low $q''_w$ that are applicable for low $u_m$, $Po \approx 64$, except in the vicinity of the inlet (Fig. 8a);

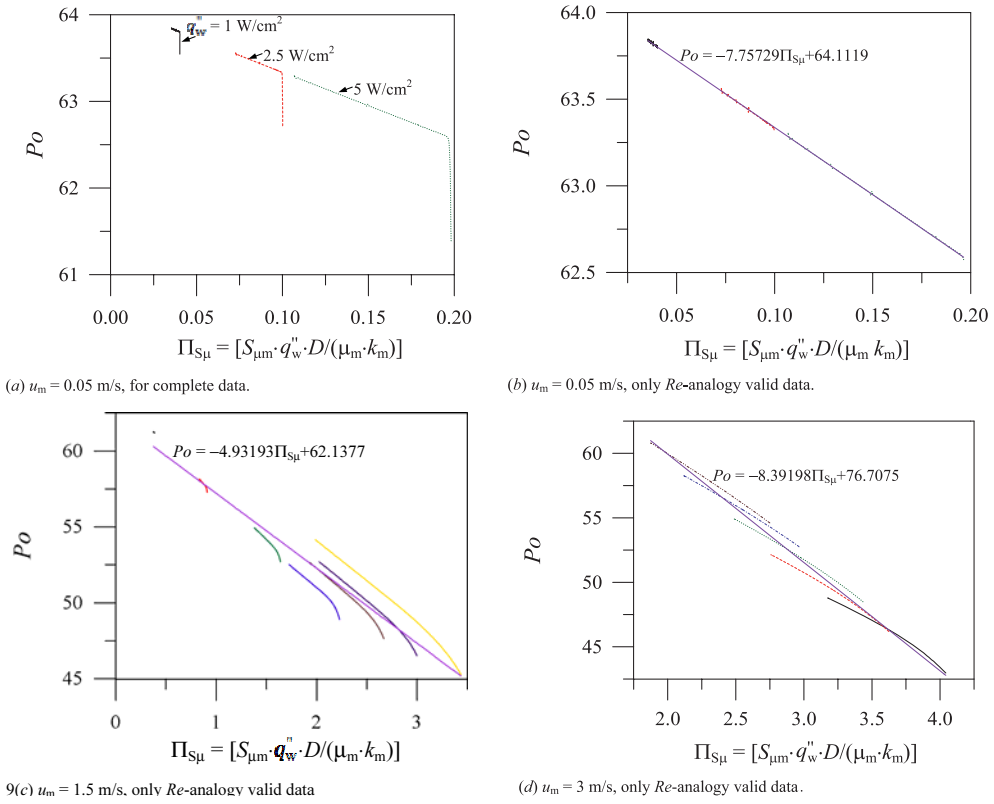


**Fig. 9.** Variation of $Po$ versus $\Pi_{S\mu}$. (a) $u_m = 0.05$ m/s, for complete data. (b) $u_m = 0.05$ m/s, only Re-analogy valid data. (c) $u_m = 1.5$ m/s, only Re-analogy valid data. (d) $u_m = 3$ m/s, only Re-analogy valid data.

but for higher $q''_w$ applicable for higher $u_m$, $Po$ deviates from 64 (Figs. 8b, 8c). Figure 9 shows the variation of the data obtained from numerical experiments on the plot of $Po$ with $\Pi_{S\mu}$, for $u_m = 0.05$ m/s, 1.5 m/s, and 3 m/s. For $u_m = 0.05$ m/s, the complete data is shown in Figure 9a, and the data for which Reynolds' analogy is valid is shown in Figure 9b. Figure 9a shows that the same trend is followed for the three different $q''_w$ in the region where the Reynolds' analogy is valid. Figures 9b–9d indicate a correlation of the numerical data; therefore, $Po$ correlates with $\Pi_{S\mu}$ in the region where the Reynolds' analogy is valid.

For large $q''_w$ that are enabled at high $u_m$, $\Pi_{Sk}$ in the energy equation [Ref. Eq. (8.1)] is also expected to affect $Po$. Its' role in $T(rz)$-variation, which determines $\mu(r, z)$-variation that affects $u(r, z)$ and $v(r, z)$ fields and $f$, should be investigated as scope for future research.

## 5 Conclusions

(i) The validity of Reynolds' analogy is determined by the inverse dependence of Reynolds number with skin friction coefficient ($c_f$). Its' validity for convective-flow with constant fluid properties results in an increasing Stanton number ($St$) with an increasing $c_f$, which is well-known. But its' validity for incompressible convective-flow with variations in fluid properties results in an increasing $St$ with a decreasing $c_f$, which is unexpected.

(ii) The Chilton-Colburn analogy of $St\,Pr^{2/3}$ increasing with increasing $c_f$ is qualitatively valid whenever the Reynolds' analogy is valid.

(iii) The Sieder-Tate's property-ratio method for obtaining Nusselt number ($Nu$) corrections has a theoretical basis, which is the validity of Reynolds' analogy.

(iv) The $Nu$ is proportional to the wall axial velocity gradient raised to the same exponent as in the Sieder-Tate correlation, when Reynolds' analogy is valid.

(v) The validity of the Reynolds' analogy is linked to the applicability of the *Theorem of Minimum Entropy Production*. The region of invalidity of the Reynolds' analogy is attributed to the phenomenon of hydrodynamic undevelopment of flow.

(vi) The Poiseuille number correlates with the dimensionless group, $\Pi_{S\mu} = Br_{S\mu}/Br_{qw} = S_{\mu m} q''_w D/(\mu_m k_m)$, in the region of validity of the Reynolds' analogy.

The authors gratefully acknowledge the full support provided by the A. von Humboldt Foundation, Germany, for this collaborative research. The authors thank Dr. Ing. O. Hausner and Dr. Ing. F. Kock, Scientific Staff at Technische Universität Hamburg-Harburg-Germany, for their support in CFD-simulations. The authors are grateful to C.A.S.D.E. Deptt. of Aerospace Engg. IIT-Bombay, for the support provided in logistics.

## References


1. E.N. Sieder, C.E. Tate, Industrial Engineering Chemistry **28**, 1429 (1936)
2. H. Herwig, Int. J. Heat Mass Transfer **28**, 423 (1985)
3. H. Herwig, M. Voigt, F.-J. Bauhaus, Int. J. Heat Mass Transfer **32**, 1907 (1989)
4. S.P. Mahulikar, H. Herwig, O. Hausner, F. Kock, Europhys. Lett **68**, 811 (2004)
5. S.P. Mahulikar, H. Herwig, Appl. Phys. Lett. **86**, 014105 (2005)
6. S.P. Mahulikar, H. Herwig, Physics of Fluids **18**, 073601 (2006)
7. S.P. Mahulikar, H. Herwig, J. Phys. D: Appl. Phys. **9**, 4116 (2006)
8. J.C. Harley, Y.F. Huang, H.H. Bau, J.N. Zemel, J. Fluid Mechanics **284**, 257 (1995)
9. K.C. Toh, X.Y. Chen, J.C. Chai, Int. J. Heat Mass Transfer **45**, 5133 (2002)
10. C. Nonino, S. Del Giudice, S. Savino, Int. J. Heat Mass Transfer **49**, 4469 (2006)
11. S.P. Mahulikar, H. Herwig, O. Hausner, IEEE/ASME J. Microelectromechanical Systems **16**, 1543 (2007)
12. G.E. Karniadakis, B.B. Mikic, A.T. Patera, J. Fluid Mechanics **192**, 365 (1988)
13. H. Schlichting, K. Gersten, *Boundary-Layer Theory*, 2nd printing, 8th edn. (McGraw Hill, New York, 2003)
14. C.J. Geankoplis, *Transport Processes and Separation Process Principles*, 4th edn. (Prentice-Hall, NJ, 2003)
15. J.P. Holman, *Heat Transfer*, 7th edn. (McGraw-Hill, London, 1990)
16. F.S. Sherman, *Viscous Flow* (McGraw-Hill, New York, 1990)
17. S.P. Mahulikar, C.P. Tso, Proceedings of the Royal Society (London) Series A: Mathematical, Physical & Engineering Sciences **458**, 669 (2002)
18. T.H. Chilton, A.P. Colburn, Industrial & Engineering Chemistry **26**, 1183 (1934)
19. A. Bejan, *Entropy Generation through Heat and Fluid Flow* (John Wiley and Sons, New York, 1982)
20. I. Prigogine, *Introduction to Thermodynamics of Irreversible Processes* (Interscience Publishers, New York, 1961)